Available online at www.sciencedirect.com
SCIENCE DIRECT®
Journal of Solid State Chemistry 173 (2003) 335–341
JOURNAL OF SOLID STATE CHEMISTRY
http://elsevier.com/locate/jssc

Synthesis and characterization of Gd_2O_3:Eu^{3+} phosphor nanoparticles by a sol-lyophilization technique

C. Louis,[a] R. Bazzi,[a] Marco A. Flores,[a] W. Zheng,[a] K. Lebbou,[a,*] O. Tillement,[a] B. Mercier,[a] C. Dujardin,[a] and P. Perriat[b]

[a] *Physical Chemistry of Luminescent Materials, Claude Bernard/Lyon University, CNRS UMR 5620, Villeurbanne, Cedex 69622, France*
[b] *UMR 5510 CNRS INSA of Lyon, France*

Received 26 September 2002; received in revised form 23 January 2003; accepted 1 February 2003

Abstract

The characterization and luminescence properties of nanostructured Gd_2O_3:Eu^{3+} phosphors synthesized by a sol-lyophilization process are presented. After preparation of gadolinium-based sols from gadolinium nitrate and ammonium hydroxide, the so-prepared sols were freeze dried at $-10°C$ and calcinated at different temperatures. For temperatures lower than 1300 K, highly crystalline samples with the cubic structure can be obtained without concomitant grain growth of the particles (<50 nm). The luminescence spectra contain all possible transitions of Eu^{3+} with C_2 symmetry and present two major features: an increase of the luminescence efficiencies of the phosphors in comparison with that obtained by solid-state reaction and the presence of an additional peak at about 609 nm at the vicinity of the $^5D_0 \rightarrow {}^7F_{0\ldots4}$ transition.

Keywords: Lyophilization; Nanoparticles; Crystalline; Phosphors; Luminescence

1. Introduction

The research of efficient and inexpensive nanoparticles is a challenging problem for the new materials generation [1–3]. The production of luminescent materials for technology applications requires strict control over their powder characteristics which include chemical homogeneity, low-impurity levels and a sub-micrometer particle size with a narrow distribution [4,5]. The conventional phosphor production through high temperature solid-state reactions typically results in particle sizes of 5–20 mm [6]. Aiming at nanometer-sized oxide particles, more advanced types of synthesis are then required [7–9]. Since the gadolinium oxide presents good luminescent properties when doped with rare-earth ions (Eu^{3+}, Tb^{3+}) [10–12], the oxide phosphor materials could be a good example to improve the luminescence properties and to extend the application field to a large domain [13,14]. The aim of this paper is to evaluate the possibility of synthesis of Gd_2O_3:Eu^{3+} sub-micrometer sized phosphors with improved luminescent properties using a sol-lyophilization technique. To obtain such nanometer-sized phosphors, low-temperature processes are preferred to those involving the comminution of samples prepared by classical solid-state reactions: indeed, only these soft processes permit to obtain samples with well-controlled composition, narrow particle size distribution and to avoid the defects generally induced by high-energy ball milling. These oxide phosphor materials could be a good example to improve the luminescence properties and to extend the application field to a large domain [15]. Such low-temperature processes have already been investigated for the preparation of nanosized phosphors in the case of yttrium-based phosphors [16,17]. They mainly consist of sol–gel techniques. However, the sol–gel processes involve precursors or solvents which contain organic parts which may induce uncontrolled grain growth during their exothermic degradation. They also suffer from the residual pollution of the samples, which strongly decreases the luminescent efficiency. Furthermore, they involve the formation of a gel whose structure may greatly influence the final particle size. Indeed, the gel in solution is characterized by an interconnected and rigid network having

*Corresponding author. Fax: +33-4-72-43-12-33.
E-mail address: lebbou@univ-lyon1.fr (K. Lebbou).

0022-4596/03/$ - see front matter © 2003 Elsevier Science (USA). All rights reserved.
doi:10.1016/S0022-4596(03)00107-5

sub-micrometer pores and polymeric chains with an average length in the micrometer range. Such a structure determines the size of the agglomerates obtained after gel drying (usually solvent evaporation between room temperature and 80–100°C). Because of strong interactions between the nanometer sized particles of the agglomerates, particles coalescence can occur during further thermal annealing leading to uncontrolled grain growth until the micrometer range. In this paper, a simple sol-lyophilization process is studied. This process avoids both the use of organic compounds and eliminates the particles agglomeration before annealing. The sols consist of dispersions of colloidal Eu-doped hydroxide nanoparticles in water. Subjected to lyophilization, the sols lead to a well-dispersed powder with a high surface area. Finally, the powders were calcinated at different temperatures with the preservation of the nanometric scale to obtain red emission phosphors.

2. Experimental

Finely divided europium-doped gadolinium oxide powder wa prepared according to the sol-lyophilization process described in Fig. 1. Gadolinium nitrate, $(NO_3)_3Gd \cdot H_2O$ and europium nitrate $(NO_3)_3Eu \cdot H_2O$ with certified purity of 99.9% from Aldrich were dissolved in water with a small amount of HCl 25%. Two europium doping concentrations have been studied: 1% and 5% in weight. With the addition of a solution of NaOH (5 M), precipitation was instantaneous and the hydroxide was formed according to the equation:

$$(1-x)Gd^{3+} + xEu^{3+} + 3\,OH^- \rightarrow ((1-x)Gd, xEu)^{3+}(OH^-)_3.$$

During the reaction, the system was continuously stirred at 800 rpm. The so-obtained precipitates were washed four times with deionized water containing a small amount of ammonia solution (pH > 10) under ultrasonication for 5 min. Each washing was followed by centrifugation at 6500 rpm for 20 min. After the fifth washing a sol was obtained, freeze dried at −10°C and dried at 400 K. The hydroxide obtained was then thermally annealed at different temperatures between 500 and 1300 K in order to obtain europium-doped gadolinium oxide.

For comparing sol-lyophilization and solid-state reactions processes, contrastive bulk material Gd_2O_3:Eu (1%) was also prepared by high-temperature sintering method (HSM). Starting materials Gd_2O_3 and Eu_2O_3 were mixed, grounded, then heat treated at 1300 K for 2 h. This procedure was repeated 5 times.

Fourier transform infrared (FTIR) spectroscopy has been carried out using a Perkin-Elmer spectrum GX spectrometer. X-ray diffraction diagrams were carried out using an D5000 Siemens diffractometer with the Cu$K\alpha_1$ and Cu$K\alpha_2$ X-rays ($\lambda = 0.15406$ and 0.15444 nm). The diffraction pattern was scanned over the 2θ range 3–50° in steps of 0.02° and a counting time of 8 s/step D5000. The parameter of the crystalline sample has been refined taking into account the aberration arising from the specimen displacement, $D_{2\theta}$, given by the formula: $D_{2\theta} = -(2\,s/R)\cos 2\theta$ where s is the displacement of the sample surface with respect to the axis of the goniometer and R the radius of the goniometer circle. Similarly, the microstrains and the size of the coherent domains have been derived from a refinement of the full-width at half-maximum (FWHM), β, of the patterns fitted with pseudo-Voigt functions according to the following relation: $\beta^2 = U\tan^2\theta + IG/\cos^2\theta$. In the latter relation, U is an estimate of the isotropic broadening due to the presence of microstrains: $\varepsilon = (\pi/1.8)\sqrt{U}$ (ε the defect concentration in %) and IG is a measure of the isotropic size effect: $T = 180\,K\lambda/\pi\sqrt{IG}$ (T the size in A, λ the wavelength in A and K the Scherrer constant here equal to $\frac{4}{3}$) [18]. The particle sizes were measured from the calcul of the FWHM of the principal peaks that belongs to the spectra of hydroxide ((100) (110) (101)) and oxide ((222) (400) (440)). The FWHM have been corrected from the instrumental corrections obtained from an annealed BaF_2 reference. High-resolution transmission electron microscopy (HRTEM) and scanning electron

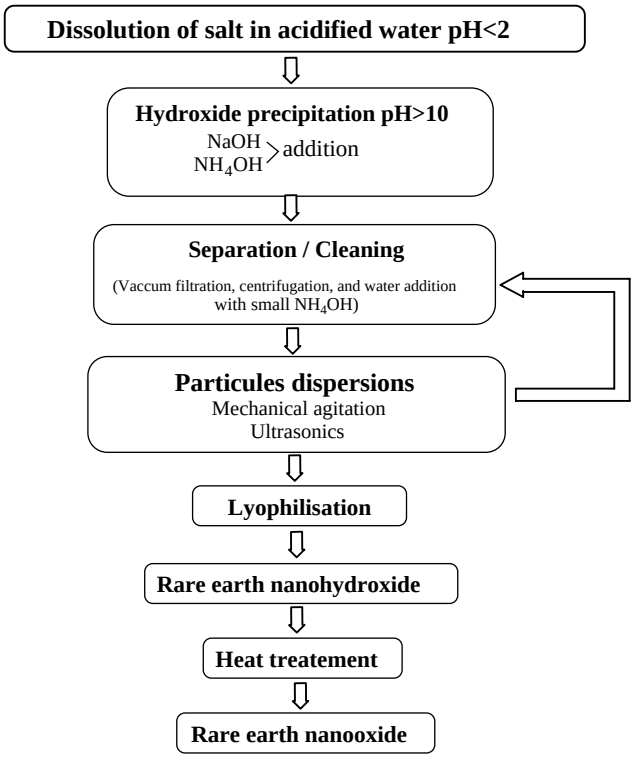

Fig. 1. Flowchart of the sol-lyophilization process for synthesis of Eu-doped Gd_2O_3 phosphor.

microscopy (SEM) were carried out using, respectively, a JEOL 2010 microscope operating at 200 kV and a Philips microscope operating at 20 kV. Fluorescence spectra were obtained using excitation with a Xe lamp and a J. Y. H10D monochromator (set at $\lambda = 250$ nm). Light was collected with an UV optical fiber coupled to a J. Y. TRIAX 320 and CCD camera (1200 g/320 nm grating, resolution = 0.65).

3. Results and discussion

Fig. 2 shows the X-ray diffraction diagram evolution of the samples during thermal annealings. The diagram

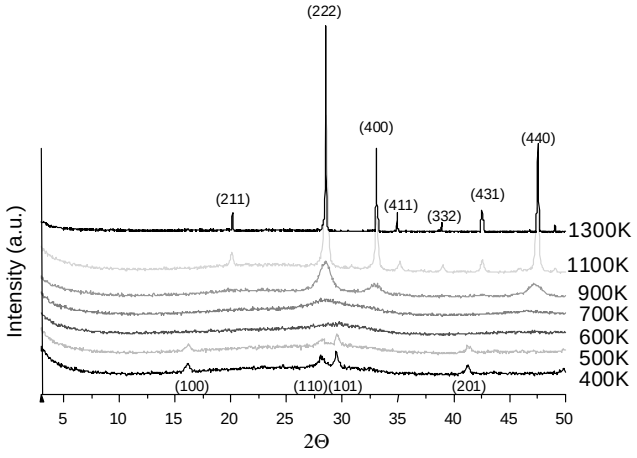

Fig. 2. Evolution of X-ray diffraction patterns of 1% europium-doped Gd_2O_3 powders during the hydroxide/oxide transformation around 600 K.

of the starting material obtained after lyophilization procedure is characterized by the superposition of (i) an important background characteristic of a non-crystalline phase and (ii) the patterns of a tetragonal structure whose cell parameters are very closed ($a = 6.35 \pm 0.01$ Å, $c = 3.63 \pm 0.01$ Å) from those corresponding to $Gd(OH)_3$ [JCPDS file 38-1042] ($a = 6.345$ Å, $c = 3.63$ Å). TEM observations of the starting material (Fig. 3) permit to make precise the morphology of the starting powders. They consist of elongated cylindrical particles with a diameter, D, around 15–20 nm and a length, L, 50–80 nm containing several zones corresponding either to crystalline or non-crystalline phases. It is then inside each particle of europium-doped gadolinium hydroxide that the amorphous and the tetragonal phases evidenced by X-ray diffraction coexist. This explains why the coherent length of the crystalline phase in the [110] direction given in Fig. 5 (3 nm for the starting sample, 15 nm for the sample heated at 400 K) is smaller than the corresponding diameter of the precipitates ($D = 15-25$ nm). During annealing of the starting material, two successive steps can be evidenced by X-ray diffraction: from room temperature up to 600 K, there is a transformation of the tetragonal phase to a non-crystalline one, from 600 to 1300 K, there is a crystallization of the sample into a cubic structure with cell parameters characteristic of gadolinium oxide C-M_2O_3 structure [19]. The fact that the material so obtained after heating is an oxide, was confirmed by FTIR spectroscopy (Fig. 4). Above 600 K, the sharp band at 560 cm^{-1} characteristic of the presence of the cubic phase of gadolinium oxide appears and becomes more pronounced when increasing the

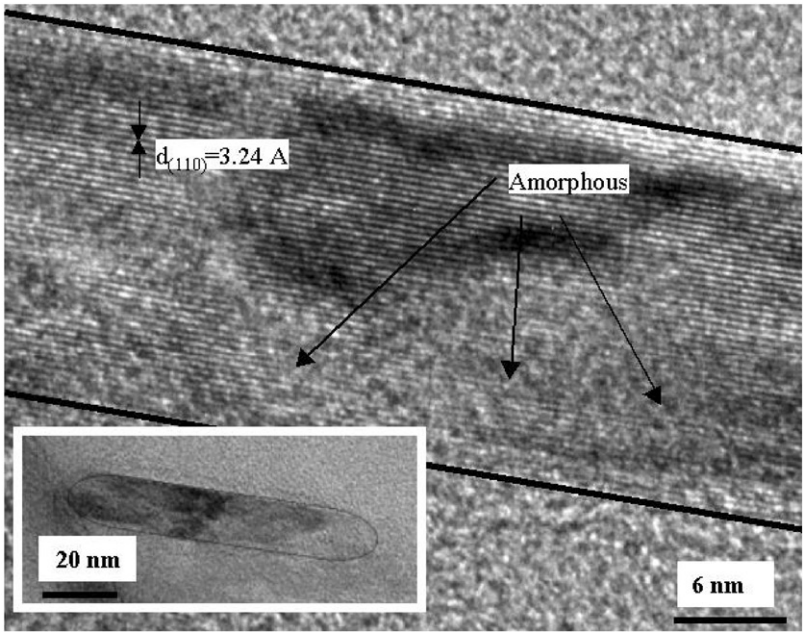

Fig. 3. TEM image of $Gd(OH)_3$ obtained from the initial lyophilization step. The dark area correspond to the best crystallized zones.

temperature. At the same time, the elimination of physisorbed species is evidenced by the progressive disappearance of the peak at 3445 cm^{-1} which arises from the absorption of O–H vibration, the peaks in the wavelength range (1400–1600 cm^{-1}) which come from the carbonate groups and a weak peak at 846 cm^{-1} due to the absorption of CO_3^{2-}. The transformation of hydroxide into oxide during thermal annealing was also confirmed by thermogravimetric measurements at a heating rate of 5°C/min up to 1300 K. Indeed, important mass losses of ≈21% noticed around 600°C correspond almost exactly to the departure of H_2O accompanying the formation of oxide from hydroxide: $2Gd(OH)_3 \rightarrow Gd_2O_3 + 3H_2O$. Such an agreement between the experimental and expected mass losses also indicates a low-impurity level in the hydroxide precipitate. Above 700 K, Fig. 5 shows that the particle size of the europium-doped gadolinium oxide increases with temperature from 3 nm at 700 K up to 40 nm at 1300 K. The particle size has been evaluated from the broadening of the diffraction peaks according to the method developed in the experimental part. In the case of the hydroxide particles whose shapes are very anisotropic (see Fig. 3), several sizes are given corresponding to the coherent length in the [110] and [101] directions. The small particle size of the oxide obtained at 700 K is confirmed (Fig. 6) by the transmission electron micrographs of the sample annealed at 700 K. Above 900 K, the grain growth is rapid before slowing down and even comes to a stop around 1100 K. Although the kinetics of the grain growth which is related to the diffusion phenomena is thermally activated (which explains the first increase of the growth rate), the size of the growing oxide particles is limited to that of the initial precipitates of hydroxide. This confirms that the lyophilization step permits to obtain hydroxide particles so separated that further coalescence between the particles is strongly limited during thermal annealing. Similarly, the crystalline content of the samples, characterized by the peak-background intensity ratio, significantly increases up to ≈100% above 1100 K. Finally, refinements of the cell parameter given in Table 1 show that the cell parameter first decreases with the annealing temperature and does not present further evolution at 1300 K. The first

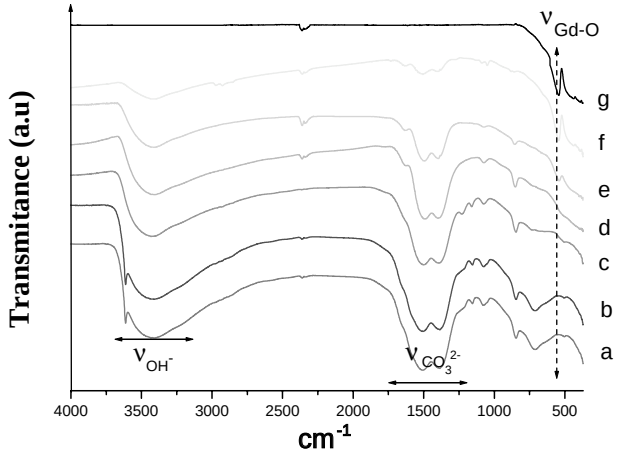

Fig. 4. Evolution of FTIR spectra of 1% europium-doped gadolinium hydroxide/oxide powders with temperature: (a) 400 K, (b) 500 K, (c) 600 K, (d) 700 K, (e) 900 K, (f) 1100 K, (g) 1300 K. Evidence for impurities elimination and formation of oxide with the cubic structure.

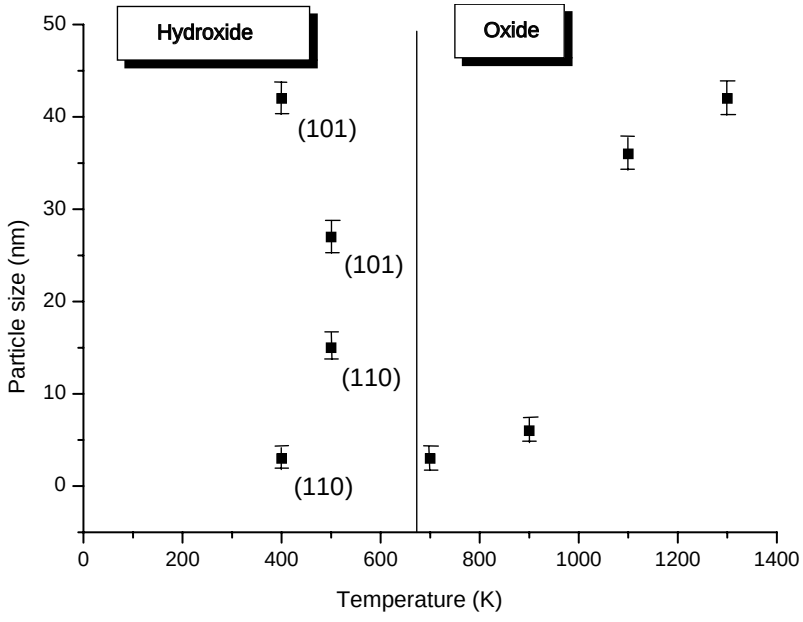

Fig. 5. Evolution of the particle size with temperature for hydroxide (below 500 K) and oxide (above 600 K). Due to the hydroxide anisotropy, several sizes are given corresponding to the coherent length in the [110] and [101] directions. Due to the presence of both crystalline and non-crystalline phases in the hydroxide precipitates, the coherent length in the [110] direction is smaller than the precipitate diameter.

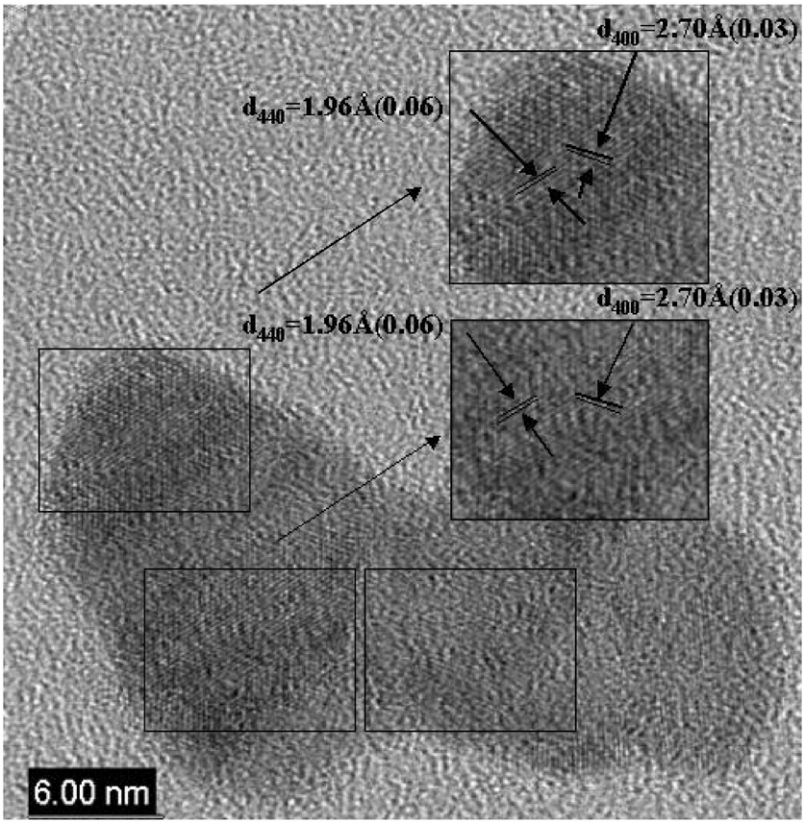

Fig. 6. TEM image of Gd_2O_3 annealed at 700 K: nucleation in the precipitate of oxide particles with a size of 3 nm. The oxide particles have been surrounded and for two of them the franges characteristic of planes of the cubic structure have been indexed.

Table 1
Evolution of the cell parameter of the cubic structure of the 1% Eu-doped gadolinium oxide with the annealing temperature

Annealed temperature (K)	Cell parameter (Å)
700	11.00 ± 0.01
900	10.87 ± 0.01
1100	10.820 ± 0.005
1300	10.808 ± 0.001

decrease corresponds to the elimination from the cubic structure of interstitial hydroxide groups evidenced from both thermogravimetric and mass spectrometer analysis. After complete water elimination, the cell parameter is equal to 10.808 ± 0.001 Å in the case of a doping content of 1% and to 10.810 ± 0.001 Å in the case of a doping content of 5%. Such values are in good agreement with those expected for gadolinium oxide (10.81 Å) and for europium oxide (10.86 Å). In the case of a Gd_2O_3/Eu_2O_3 solid solution, the difference between the cell parameters of the two differently doped samples would be equal to 0.002 Å which is in agreement with that found experimentally. Despite the uncertainties of the cell parameters, this would confirm the existence of a solid solution between the two rare-earth oxides. Finally, the defect concentrations due to the presence of microstrains inside the particles are very low: 0.8% in the case of the 1% doped oxide and 0.6% in the case of the 5% doped one. Then it can be concluded that, contrary to processes involving solid-state reactions, only moderate temperature annealings (1300 K) yield samples which are simultaneously highly crystallized, nanometer-scaled and free of chemical and morphological defects.

The emission properties of 1% europium-doped rare earth-doped phosphor materials as a function of annealing temperature are given in Fig. 7. Detectable red emission of samples annealed at temperatures lower than 600 K is shown in the inset of Fig. 7. Such an emission is characterized by three unresolved broadbands and correspond to that of $Gd(OH)_3$:Eu. When increasing annealing temperature the broadbands sharpen and turn to typical emission of Eu^{3+} with C_2 and S_6 symmetry corresponding to the 24*d* and 8*a* sites in bcc Gd_2O_3, respectively. Four groups of distinctive emission peaks between 575 and 660 nm are related to the $^5D_0 \rightarrow {}^7F_j$ ($j = 0, 1, 2, 3$) transitions of Eu^{3+}, respectively. Their intensities increase with the annealing temperature due to the high crystalline content of the particles (Fig. 6). The first important information in the spectra data of the nanostructured powders consists of a surprising additional peak at about 609 nm at the vicinity of the $^5D_0 \rightarrow {}^7F_2$ transition (C_2 site). Such a

peak, evidenced for the first time, is more pronounced for the oxide with the lower particle size: indeed, the intensity ratio of this peak to the 611 nm line (the main peak of $^5D_0 \rightarrow {}^7F_2$ transition in bcc Gd_2O_3:Eu) decreases when increasing the temperature. In the sample annealed at 1300 K with a particle size of $\approx$40 nm, the luminescence spectral becomes a classical phosphor cubic Gd_2O_3 oxide. It is then clear that this peak is size dependent; it may be assumed that this 609 nm peak is the emission from Eu^{3+} states that modified the surface, whereas the 611 nm peak corresponds to that rising from Eu^{3+} in a well-crystalline core. The presence of the 609 nm peak is confirmed by the results shown in Fig. 8. Fig. 8 (left) is the excitation spectra of Gd_2O_3:Eu with a particle size of 3 nm. The charge transfer (CT) band shifts from 247 nm for 611 nm emission to 258 nm for 609 nm emission, which named by CTc and CTs, respectively. When exciting sample at 220 nm, which means only exciting the Eu^{3+} ions in core, we obtain the well-known emission spectrum for bcc Gd_2O_3:Eu (curve 1 on the right of Fig. 8). Then exciting sample at 270 nm, because of the overlap of CTc and CTs all of the Eu^{3+} ions can be excited, but the excitation of the Eu^{3+} state surface ions is more efficient. As expected, the 609 nm peak is more intense in this case as shown by curve 2 in Fig. 8 (right). Other obvious differences in spectral distribution between 590–595 nm and 620–635 nm are under further investigation. Measures of decays were carried out from the emission lines at 609 and 611 nm (surface and core peak, respectively). The results are similar compared to bulk materials. Nevertheless, a slight no-experimental profile was observed for the 609 fluorescence line. A second important information can be drawn from the spectral comparison of samples obtained from different elaboration routes (Fig. 9). Indeed the luminescent efficiency of the sample prepared from sol-lyophilization process and annealed only 2 h at 1300 K is 7 times higher than that obtained by solid-state reaction performed at the same temperature for 10 h. In order to compare the light output, the same excitation wavelength as well as same light collection setup has been used from sample to sample. The

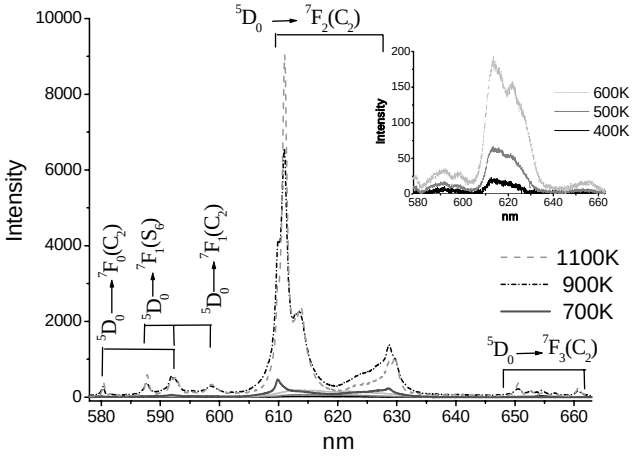

Fig. 7. Emission spectra of Gd_2O_3:Eu(1%) phosphors annealed from 700 to 1300 K, excited at 250 nm. Inset: emission spectra of samples annealed from 400 to 600 K.

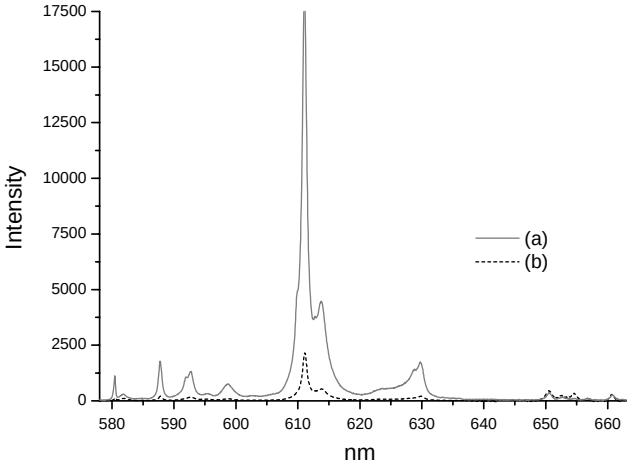

Fig. 9. Room temperature emission spectra of phosphor powders Gd_2O_3:1%Eu annealed at 1300 K excitated at $\lambda = 250$ nm. Comparison of sol-lyophilization route (a) and solid-state reactions process (b).

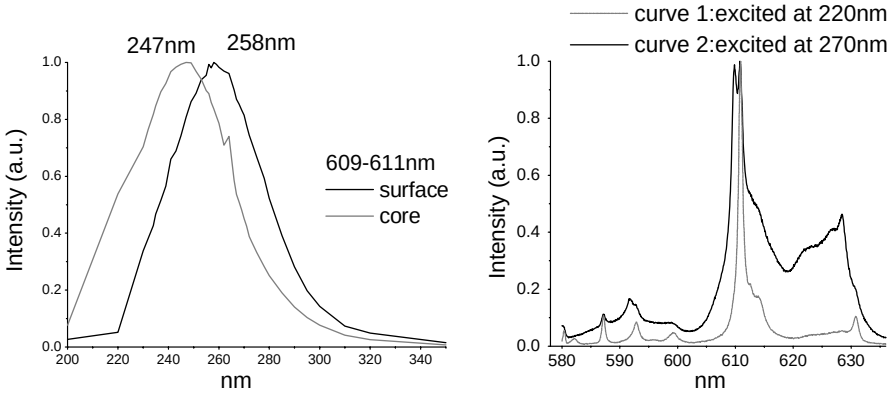

Fig. 8. Excitation spectra of Gd_2O_3:Eu(1%) with a particle size of 3 nm (left) and emission spectra of the same sample (right) excited at 220 nm (curve 1) and at 270 nm (curve 2).

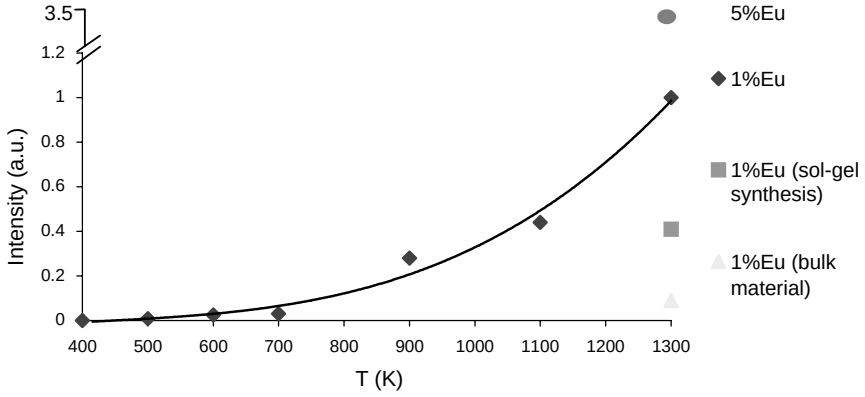

Fig. 10. Emission intensity ($\lambda_{exc} = 250$ nm) as function of temperature, ratio doping and process. The value for the sol–gel process has been derived from Ref. [17] indicating an increase of 20% of the emission intensity compared with that obtained in the case of solid state reactions route.

increased efficiency of the activator Eu^{3+} cations in the powders is probably due to the chemical homogeneity and to the nanometer scale of the particles. Fig. 10 details the increase of the luminescent efficiency with the temperature of annealing and provides deeper comparison with the samples obtained from other processes. When increasing the temperature, the crystalline content increases whereas the increase of the particle size is limited to the size of the freeze-dried precipitates (≈ 40 nm). This explains why an increase of the doping content of 5% enables a correlative increase of the luminescent intensity as high as 3.5%, and also why the luminescent efficiency of the powders prepared from the sol-lyophilization process is much higher than that of the samples obtained from the sol–gel processes. In the sol–gel route indeed, the formation of a gel which is structured at the micrometer scale leads, after annealing, to a much greater final particle size $\approx 1\,\mu$m.

4. Conclusion

Eu-doped Gd_2O_3 phosphor particles with red emission light have been successfully prepared using the sol-lyophilization technique. This process is suitable for obtaining nanostructured phosphor with high degrees of crystalline phases and low process induced contaminations. In comparison with classical solid-state processes and even sol–gel routes, improved luminescence properties have been found. The possibility of obtaining for the first time, a powder with a narrow particle distribution around 3 nm also permitted to evidence an additional peak in the luminescence spectra. This peak has to be probably related to the size effect since it disappears when the size increase. To precise this point, more studies concerning the grain size dependence of the luminescence properties are in progress and will be given later.

In particular, the present work emphasizes the interest of preparing colloids for better characterization of 609 nm emission line. If such a line was indeed related to the Eu^{3+} on/near the surface, it could be easily checked by changing the solvent and then the refractive index of the colloidal stable solution.

References

[1] L.E. Brus, L.W. Brown, R. Andres, S.R. Averback, A.W. Goddard, A. Kaldor, G.S. Louie, M. Moskovits, S.P. Peercy, J.S. Reley, W.R. Siegel, A.F. Spaepen, Y. Wang, J. Mater. Res. 4 (1989) 704.
[2] V.A. Alexandria, Research Opportunities for Materials with Ultrafine Microstructures, National Academy Press, Washington DC, 1989.
[3] Science 254 (1991) 1300.
[4] S. Shikao, W. Jiye, J. Alloys Compds. 327 (2001) 82–86.
[5] K.E. Gonsalves, G. Carlson, J. Kumar, F. Aranda, M.J. Yacama, in: Gan-Moog Chow, K.E. Gonsalves (Eds.), Symposium sponsered by the Division of Polymeric Materials: Science and Engineering, Inc. at the 210th National Meeting of the American Chemical Society, Chicago, IL, August 20–24, 1995.
[6] E. Giannelis, in: Gan-Moog Chow, K.E. Gonsalves (Eds.), Nanotechnology Molecularly Designed Materials, 1995.
[7] A.D. Yoffe, Adv. Phys. 42 (1993) 173.
[8] R.N. Bhargava, D. Gllagher, Phys. Rev. Lett. 72 (1994) 416.
[9] C.R. Ronda, J. Lumin. 72–74 (1997) 49–54.
[10] E. Zych, Opt. Mater. 16 (2001) 445–452.
[11] C.J. Summers, IDW'96 Proceedings, Vol. 2, November 18–20, 1996, p. 13.
[12] Aron Vecht, Extended Abstracts of Second International Conference on the Science and Technology of Display Phosphors, San Diego, CA, November 18–20, 1996, p. 247.
[13] L. Sun, J. Yao, C. Liu, C. Liao, C. Yan, J. Lumin. 87–89 (2000) 447–450.
[14] Y.L. Soo, S.W. Huang, Y.H. Kao, V. Chhabra, B. Kulkami, J.V.D. Veliadis, R.N. Bhargava, Appl. Phys. Lett. 75 (1999) 2464–2466.
[15] N. Millot, S. Begin Colin, P. Perriat, G. Le Caer, J. Solid State Chem. 139–1 (1998) 66–78.
[16] R.P. Rao, J. Electrochem. Soc. 143–1 (1996) 189–197.
[17] J. Zhang, Z. Zhang, Z. Tang, Y. Lin, Z. Zheng, J. Mater. Process. Technol. 5622 (2002) 1–4.
[18] J.B. Langford, Aust. J. Phys. 41 (1988) 173–187.
[19] A.FD. Wells (Ed.), Structural Inorganic Chemistry, Oxford Science Publications, Oxford, p545C.